Gramian-based Characterization of Network Vulnerability to Nodal Impulse Inputs

Prasad Vilas Chanekar*, Bala Kameshwar Poolla, Jorge Cortés

Abstract— **Impulsive inputs applied at influential nodes of a network system may result in undesirable behavior and degrade performance. This paper proposes the notion of vulnerability matrix (VM) to characterize the effect of impulse inputs on a network following either discrete-time or continuous-time dynamics. The VM describes the first-order effects of impulse inputs on edge flows and is based on the controllability Gramian. We provide explicit expressions for the elements of the vulnerability matrix for the class of directed line networks in terms of the edge weights. Simulations validate our results and highlight the utility of the proposed metric in capturing the transient effects of nodal impulse inputs on edge flows.**

I. Introduction

Complex networks are critical components of modern society touching almost every aspect of daily life. We encounter them in social dynamics, intelligent transportation, water distribution systems, biological systems, energy systems, and robotics. Networks can be mathematically modeled as graphs using nodes and edges [1], [2]. Inputs are applied at the nodes and get propagated across the network through flows on the edges, whose capacity is often constrained. The edge flows may represent various physical quantities depending upon the application, e.g., power (in energy networks), traffic (in transportation systems), or information (in communication networks). The ability to alter the network behavior through nodal inputs and their propagation through capacity-constrained edges depends on the network topology as well as its dynamics. Malicious inputs at influential nodes can result in large undesirable changes in edge flow characteristics and lead to network failures. Such influential nodes are ideal for adversarial attacks and make the network vulnerable. This paper develops formal tools to identify influential nodes by looking at the effect of impulse inputs on edge flows.

Literature review: The relative importance of a node/edge in a complex network with respect to a given metric is quantified by the notion of centrality [3]–[5]. Centrality can depend on many factors, including the network topology and the inherent dynamical properties of the nodes and interconnections. An exhaustive list of centrality measures is available in the introduction of our previous work [6]. Network centrality has been traditionally studied purely from a topological perspective. Works from the controls literature, e.g., [7]–[9] and references therein, instead look at the combined effect of network topology and the underlying dynamics. In [10], novel measures based on the controllability and observability Gramians are proposed to quantify the influence of each node on the rest of the network and vice-versa. A Gramian-based vulnerability analysis of networks, with respect to coordinated attacks on network links and manipulated data injections is presented in [11]. The work [12] proposes a novel security index to quantify the effect of attack inputs injected by an adversarial agent on the outputs and states of a network system. The work [13] employs the $\mathscr{H}_2-$system norm as a measure to characterize robustness properties and fundamental limits of dynamical networks against external distributed stochastic disturbances. [14] presents novel measures based on the $\mathscr{H}_2-$system norm for linear networks with noisy nodal inputs to identify vulnerable nodes and interconnections. The work [15] characterizes the response of the network to external stimuli or parameter changes by the network's fragility, computed using the stability radius. Thus, in general, for dynamical network systems, vulnerability analysis have been attempted in terms of the system's (abstract) structural properties (controllability, observability, or stability radius). On the other hand, the study of flow vulnerabilities in dynamical networks is mainly focused on the analysis of sequence of steady states, e.g., [16]. The work [17] provides an analytical study of network susceptibilities quantifying the response of the dynamics to small parameter changes. Finally, [18] shows that network components may fail due to the transients arising from the dynamics, something often overlooked by the analysis of sequential steady states. Note that the relationship between Gramian-based vulnerability metrics and the change in network flows is not present in the aforementioned literature.

Statement of contributions: We consider networks described either by linear discrete-time or continuous-time dynamics with scalar states. The information regarding the nodal interconnections is captured by the network's weighted adjacency matrix. Our treatment requires the network dynamics to be stable and has no restriction on the structure of the adjacency matrix. Our first contribution pertains to the derivation of analytical expressions of the evolution of

This work was partially supported by AFOSR Award FA9550-19-1-0235.

Prasad Vilas Chanekar (*corresponding author) is with the Department of Electronics and Communication Engineering, Indraprastha Institute of Information Technology, New Delhi, India 110020, prasad@iiitd.ac.in, Bala Kameshwar Poolla is with the National Renewable Energy Laboratory, Golden CO 80401, USA, bpoolla@nrel.gov, Jorge Cortés is with the Department of Mechanical and Aerospace Engineering, University of California, San Diego, La Jolla, CA 92093, USA, cortes@ucsd.edu

This work was authored by the National Renewable Energy Laboratory, operated by Alliance for Sustainable Energy, LLC, for the U.S. Department of Energy (DOE) under Contract No. DE-AC36-08GO28308. Funding provided by NREL Laboratory Directed Research and Development Program. The views expressed in the article do not necessarily represent the views of the DOE or the U.S. Government. The U.S. Government retains and the publisher, by accepting the article for publication, acknowledges that the U.S. Government retains a nonexclusive, paid-up, irrevocable, worldwide license to publish or reproduce the published form of this work, or allow others to do so, for U.S. Government purposes.

edge flows over a time horizon after the application of an impulse input at a node. We show that the first-order effects of impulse inputs on edge flows can be written in terms of the controllability Gramian. Based on this observation, we introduce the concept of vulnerability matrix (VM). The VM quantifies the influence of each node on the edge flows when an impulse nodal input is applied, thereby helping to identify network vulnerabilities. Our analysis captures the transient effects of impulse inputs, which are often missed when only sequential steady states are analyzed. Our second contribution focuses on the class of directed line networks with positive edge weights and stable dynamics. We provide expressions for the elements of the controllability Gramian, which in turn helps us explicitly describe the elements of the VM. Our numerical simulations show that nodal influence rapidly decreases as one moves away from the input node. We also illustrate our results on a family of stable 7-node directed line networks and 1000 random Erdős-Rényi networks. These examples also highlight the application of our proposed theory in the case of networks having one dominant directed line.

II. Preliminaries

Consider[1] a network consisting of n nodes and scalar states represented by the triplet $\mathcal{G}_A = (\mathcal{V}, \mathcal{E}_A, w_A)$, where $\mathcal{V} = \{1, 2, \ldots, n\}$ is the node set, $\mathcal{E}_A = \{(i,j) \mid i \in \mathcal{V}, j \in \mathcal{V}\}$ is the edge set with cardinality n_e, and $w_A : \mathcal{E}_A \mapsto \mathbb{R}$ is a weight function. The pair (i,j) denotes an edge directed from node i to node j, i.e., $i \to j$. The weighted adjacency matrix $A \in \mathbb{R}^{n\times n}$ is defined by $a_{ji} = w_A(i,j) \neq 0$ if $(i,j) \in \mathcal{E}_A$, else $a_{ji} = 0$. The network dynamics are linear and either discrete or continuous time-invariant as follows,

$$x(t+1) = Ax(t) + b_k u\,\delta(t), \quad t \in \{0, \ldots, T-1\}, \tag{1a}$$

$$\dot{x} = Ax(t) + b_k u\,\delta(t), \quad t \geq 0, \tag{1b}$$

where t denotes time/iteration, $T > 0$ is a finite time horizon, $x \in \mathbb{R}^n$, $u \in \mathbb{R}$ is the magnitude of the impulse applied at node k at $t = 0$ with location denoted by the input vector $b_k = \bar{e}_k$. We define the output for the dynamics (1) along the edge $i \to j$ at time t as,

$$y_{ij} = c_{ij}(x_i - x_j), \tag{2}$$

where $c_{ij} \in \mathbb{R}$ is a known constant. Note that $y_{ij} \in \mathbb{R}$ in (2) indirectly depends on u through x, due to the dynamics (1). We assume the system dynamics (1) to be stable, i.e., $\text{srad}(A) < 1$ for discrete-time dynamics (1a) and $\mathcal{R}\big(\lambda_i(A)\big) < 0$ for continuous-time dynamics (1b) for all $i \in \{1, 2, \ldots, n\}$. We consider an initial state $x(0) = x_0$. The output defined in (2) is often used as a metric to measure network edge flows [17], [19] and is relevant in network theory. In power networks, for e.g., the matrix A is a Laplacian, the choice $c_{ij} = a_{ji}$ represents the line susceptance, and x the vector of bus voltage angles. The metric (2) represents the active power flow on the line [19] using the DC power flow approximation at 1 p.u. voltage. Disturbances such as lightning strikes, electrostatic discharges, and utility fault clearing, among others, can be modeled as impulses. So it is of interest to analyze the effect of disturbances on edge flows as these are often capacity constrained.

[1]Let $\mathbb{R}$ and $\mathbb{C}$ denote the set of real and complex numbers, respectively. For $x \in \mathbb{R}$ (resp. $x \in \mathbb{C}$), $|x|$ denotes its absolute value (resp. magnitude). The real part of $x \in \mathbb{C}$ is denoted by $\mathcal{R}(x)$. For $j \in \{1, \ldots, n\}$, $\bar{e}_j \in \mathbb{R}^n$ is the j^{th} canonical unit vector (the bar is used to distinguish from exponential e). $\delta(t)$ denotes the Dirac delta function. The transpose of a vector or matrix is denoted by $(\cdot)^\top$. For a vector $x \in \mathbb{R}^n$, x_i denotes its i^{th} coordinate. Given a matrix M, we denote its $(i,j)^{\text{th}}$ element by m_{ij} (or $m_{i,j}$). For a square matrix N, we use $\lambda(N)$ to denote the vector of eigenvalues, and $\text{srad}(N)$ for its spectral radius.

k	Y_{12}	Y_{13}	Y_{25}	Y_{35}	Y_{41}	Y_{43}	Y_{54}	$\sum Y_{ij}$
1	5.6	4.9	4.5	3.9	4.2	2.9	0.5	26.5
2	5.6	4.2	5.6	4.5	3.0	3.0	5.0	31.0
3	2.4	4.9	4.5	5.6	3.0	4.2	5.0	29.7
4	3.4	5.9	5.4	5.0	4.2	4.2	6.3	34.4
5	3.0	5.3	5.6	5.6	3.8	3.8	6.3	33.4

TABLE I: Max absolute flow deviation along edge $i \to j$ due to input at k.

Example 1 (Exhaustive computation of flow deviations)**.** The following example provides a motivation for our study. Consider a 5-node network as shown in Fig. 1, following a discrete-time dynamics with $x_0 = 0$. For each node, we apply an impulse input of magnitude $u = 7$ at $t = 0$ and analyze the resulting flows. The system departs from the state x_0, causing

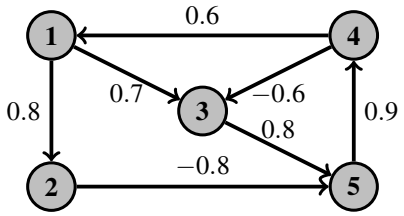

Fig. 1: A 5−node network with edge weights as indicated.

a change in flow on each edge. As $\text{srad}(A) = 0.77 < 1$, the dynamics is stable and the system returns back to the state x_0. We run the dynamic simulation for $T = 250$ iterations and choose c_{ij} in (2) as the weight of the edge $i \to j$. We record the maximum absolute flow deviation Y_{ij} on each edge due to the impulse nodal inputs in Table I, where $Y_{ij} = \max_{t\in[0,\,250]} |y_{ij}|$. To quantify the impact of an impulse at a particular node on the network, we sum the maximum absolute flow deviations as $\sum Y_{ij}$. From the numerical simulation results, we observe that an impulse at node 4 has the maximum impact, while that at node 1 has the least impact. Carrying out such simulations to observe the effect of impulse nodal inputs is inexpensive because the size of the considered network is relatively small and the magnitude of the input is known. However, in real-world applications, the network size is generally large and we may also not know the magnitude of the impulse. This makes the simulation route computationally intensive and non-robust. This motivates the introduction of metrics to quantify the effect of impulse nodal inputs on edge flows without the knowledge of the input magnitude. •

III. The Vulnerability Matrix

In this section, we present a novel metric which not only uses the network's topological properties but also its inherent

dynamics to characterize the effect of impulse nodal inputs on edge flows. To this end, we first derive an analytical expression for the evolution of edge flows for impulse inputs/disturbances.

Lemma 2. *(Analytical expressions for evolution of flow). Consider the discrete-time/continuous-time network dynamics* (1)*. If an impulse input $u \in \mathbb{R}$ is applied at node k at $t = 0$, then the evolution of the flow F_{ij} on the edge $i \to j$ defined by the output* (2) *with $x(0) = x_0$ is given by*

1) *For discrete-time dynamics,*
   $F_{ij}(t)|^k = c_{ij}(\bar{e}_i - \bar{e}_j)^\top A^{t-1}(Ax_0 + \bar{e}_k u)$, *for* $t \geq 1$,
2) *For continuous-time dynamics,*
   $F_{ij}(t)|^k = c_{ij}(\bar{e}_i - \bar{e}_j)^\top e^{At}(x_0 + \bar{e}_k u)$, *for* $t \geq 0$.

Proof. For *(i)*, the state evolution in response to an impulse input at node k can be expressed as, cf. [20],

$$x(t) = A^t x(0) + A^{t-1} b_k u, \text{ for } t \geq 1. \tag{3}$$

With the initial state $x(0) = x_0$, $b_k = \bar{e}_k$, the edge flow (2), coupled with $x_i = \bar{e}_i^\top x$, $x_j = \bar{e}_j^\top x$ yields the result.

For *(ii)*, the state evolution is given by

$$x(t) = e^{At} x_0 + \int_0^t e^{A(t-\tau)} \bar{e}_k u \, \delta(\tau) \, \mathrm{d}\tau. \tag{4}$$

As the input at time $t = 0$ is an impulse, we have from [21],

$$\int_0^t e^{A(t-\tau)} \bar{e}_k u \, \delta(\tau) \, d\tau = u e^{At} \bar{e}_k.$$

Substituting $x_i = \bar{e}_i^\top x$, $x_j = \bar{e}_j^\top x$ in (2), yields the result. □

In what follows, we use the notation ' $|^k$ ' to indicate the impulse input at node k. Next, we analyze the first-order effects of impulse nodal inputs on the network and compute the relevant analytical expressions.

Theorem 3. *(First-order effect of impulse inputs on states and edge flows). Consider the discrete-time/continuous-time network dynamics in* (1)*. If an impulse input of magnitude $u \in \mathbb{R}$ is applied at node k at $t = 0$, then*

1) $\sum_{t=0}^{\infty} \left(\frac{\partial x_i}{\partial u}\right)^2 \Big|^k = \mathscr{W}_{ii}^k = \int_0^\infty \left(\frac{\partial x_i}{\partial u}\right)^2 \Big|^k \mathrm{d}t,$
2) $\sum_{t=0}^{\infty} \left(\frac{\partial F_{ij}}{\partial u}\right)^2 \Big|^k = c_{ij}^2(\mathscr{W}_{ii}^k + \mathscr{W}_{jj}^k - 2\mathscr{W}_{ij}^k) = \int_0^\infty \left(\frac{\partial F_{ij}}{\partial u}\right)^2 \Big|^k \mathrm{d}t,$

where $\mathscr{W}^k$ is the discrete-time/continuous-time controllability Gramian with only one input at node k.

Proof. First, we consider *(i)* under the discrete-time dynamics. We recall from (3) in Lemma 2 that

$$x_i = \bar{e}_i^\top A^t x_0 + \bar{e}_i^\top A^{t-1} b_k u, \text{ for } t \geq 1.$$

Differentiating with respect to the input variable u and noting that $b_k = \bar{e}_k$ for the nodal input location, we have

$$\frac{\partial x_i}{\partial u} = \bar{e}_i^\top A^{t-1} \bar{e}_k, \text{ for } t \geq 1.$$

Note that $\frac{\partial x_i}{\partial u} = 0$ for $t = 0$. To evaluate the overall impact over time, we compute the sum from $t = 1$ to ∞, and obtain

$$\sum_{t=0}^{\infty} \left(\frac{\partial x_i}{\partial u}\right)^2 = \sum_{t=0}^{\infty} (\bar{e}_i^\top A^t \bar{e}_k)^2 = \sum_{t=0}^{\infty} \bar{e}_i^\top A^t \bar{e}_k \bar{e}_k^\top A^{t\top} \bar{e}_i.$$

Finally, using the definition of the discrete-time controllability Gramian [20] for the input matrix $\bar{e}_k$,

$$\sum_{t=0}^{\infty} \left(\frac{\partial x_i}{\partial u}\right)^2 = \bar{e}_i^\top \Big(\sum_{t=0}^{\infty} A^t \bar{e}_k \bar{e}_k^\top A^{t\top}\Big) \bar{e}_i = \bar{e}_i^\top \mathscr{W}^k \bar{e}_i = \mathscr{W}_{ii}^k.$$

For the continuous-time dynamics, we proceed similarly as above. Using the relation (4), $b_k = \bar{e}_k$, and differentiating

$$\frac{\partial x_i}{\partial u} = \bar{e}_i^\top e^{At} \bar{e}_k.$$

Next, with the integral relation below

$$\int_0^\infty \left(\frac{\partial x_i}{\partial u}\right)^2 \mathrm{d}t = \int_0^\infty (\bar{e}_i^\top e^{At} \bar{e}_k)^2 \mathrm{d}t,$$

applying suitable algebraic manipulations and the definition of the continuous-time controllability Gramian [20] for the input matrix $\bar{e}_k$, we get the required result.

For *(ii)*, under the discrete-time dynamics, note that differentiating (2) with respect to the input u results in

$$\frac{\partial F_{ij}}{\partial u} = c_{ij}\Big(\frac{\partial x_i}{\partial u} - \frac{\partial x_j}{\partial u}\Big).$$

Squaring and evaluating the summation with respect to t from 0 to ∞, we obtain

$$\frac{1}{c_{ij}^2} \sum_{t=0}^{\infty} \left(\frac{\partial F_{ij}}{\partial u}\right)^2 = \sum_{t=0}^{\infty} \left(\frac{\partial x_i}{\partial u}\right)^2 + \sum_{t=0}^{\infty} \left(\frac{\partial x_j}{\partial u}\right)^2 - 2\sum_{t=0}^{\infty} \frac{\partial x_i}{\partial u} \frac{\partial x_j}{\partial u}.$$

We can compute the last term in the expression as

$$\begin{aligned} \sum_{t=0}^{\infty} \frac{\partial x_i}{\partial u} \frac{\partial x_j}{\partial u} &= \sum_{t=0}^{\infty} \bar{e}_i A^t \bar{e}_k \bar{e}_j A^t \bar{e}_k = \bar{e}_i^\top \Big(\sum_{t=0}^{\infty} A^t \bar{e}_k \bar{e}_k^\top A^{t\top}\Big) \bar{e}_j \\ &= \bar{e}_i^\top \mathscr{W}^k \bar{e}_j = \mathscr{W}_{ij}^k. \end{aligned}$$

The result now follows from *(i)*. The proof for the continuous-time dynamics is analogous. □

If $i \to j$ is the q^{th} edge in the set $\mathscr{E}_A$, then for an impulse input u at node k, we define

$$\gamma_{kq} = \gamma_{ij}^k := \sum_{t=0}^{\infty} \left(\frac{\partial F_{ij}}{\partial u}\right)^2 \Big|^k = \int_0^\infty \left(\frac{\partial F_{ij}}{\partial u}\right)^2 \Big|^k \mathrm{d}t,$$

which are computed using Theorem 3. By collecting all such γ_{kq} for $1 \leq k \leq n$ and $1 \leq q \leq n_e$, we get a matrix $\Gamma = (\gamma_{kq}) = (\gamma_{ij}^k) \in \mathbb{R}^{n \times n_e}$. We refer to this matrix as the '*Vulnerability Matrix*' (VM). The k^{th} row of VM captures the effect of an impulse input at node k on the edge flow in each edge of the network. Instead, the q^{th} column in VM represents the effect of an impulse input (applied one at a time) at each node of the network on the q^{th} network edge. The sum $\sum_{q=1}^{n_e} \gamma_{kq}$ of the k^{th} row elements encodes the influence of the k^{th} input on all the edge flows. This is referred to as the vulnerability influence of node k and denoted by ν_k. Higher values of ν_k make node k a potential site for nodal impulse attacks (when

viewed from an adversarial viewpoint). An alternative notion, which is not explored here for lack of space, is defining vulnerability of a particular edge under impulse attacks at all nodes by summing columns of VM, i.e., $\sum_{k=1}^{n} \gamma_{kq}$.

From [7], [8], the controllability Gramian is related to the average controllability of the system, when computed along all directions of the state space. This also corresponds to the energy in the output response to a unit impulse input [6], [22]. Thus, Theorem 3 presents an energy-based expression in terms of the controllability Gramian which quantifies the effect of impulse nodal inputs on edge flows. As we assume the system matrix A is stable, we can compute the controllability Gramian using the Lyapunov equations [20] with input only at the node k as the solution to

$$\text{discrete-time:} \quad A\mathscr{W}^k A^\top - \mathscr{W}^k = -\bar{e}_k \bar{e}_k^\top, \tag{5a}$$

$$\text{continuous-time:} \quad A\mathscr{W}^k + \mathscr{W}^k A^\top = -\bar{e}_k \bar{e}_k^\top. \tag{5b}$$

IV. Edge Flow Vulnerabilities in Directed Line Networks

In this section, we characterize the vulnerability of edge flows in a network in terms of its structure. To this end, we need to express the controllability Gramian in terms of the edge weights. The analysis is complex for general networks, so we focus our attention on the particular class of directed line networks, cf. [23]. A directed line network is a sequential arrangement of nodes, e.g., starting at node 1 and ending at node n (see Fig. 2). The presence of self-loops ensures the stability of the continuous-time network dynamics. In our analysis presented next, we first study the discrete-time instance, followed by the continuous-time version.

A. Discrete-Time Directed Line Networks

Consider the directed line networks with no self-loops (i.e., $a_{ii} = 0$ for all $i \in \{1,\dots,n\}$) and with positive edge weights (i.e., $a_{ji} > 0$). The directed line networks with no self-loops following discrete-time dynamics yield a diagonal controllability Gramian [6], [23], which can be expressed in terms of their edge weights. Therefore, we can derive an analytical expression for the edge flow vulnerabilities in terms of the network edge weights. We first define the notation

$$\rho_{ij} \coloneqq a_{i+1,i}\, a_{i+2,i+1} \dots a_{j-1,j-2}\, a_{j,j-1} = \prod_{r=i+1}^{j} a_{r,r-1},$$

for $i < j$ and the directed line path $i \to i+1, \dots, j-1 \to j$ between the node i and node j. If $i = j$, then $\rho_{ii} = 1$. Notice that for $i < y < j$ with the directed line path $i \to y \to j$, we have $\rho_{ij} = \rho_{iy}\rho_{yj}$. From [6], [23], we can write the diagonal elements of the controllability Gramian for input node k as

$$\mathscr{W}_{ii}^k = 0 \text{ for } 1 \le i \le k-1 \text{ and } \mathscr{W}_{ii}^k = \rho_{ki}^2 \text{ for } k \le i \le n. \tag{6}$$

Next, we provide expressions for edge flow vulnerabilities.

Theorem 4. *(Edge flow vulnerability for directed line networks with discrete-time dynamics). Consider a directed line network of n nodes with stable discrete-time dynamics* (1a) *with positive edge weights and input node k. Then*

$$\gamma_{i,i+1}^k = \begin{cases} 0 & \text{for } 1 \le i \le k-2, \\ c_{k-1,k}^2 & \text{for } i = k-1, \\ c_{i,i+1}^2 \left(1 + a_{i+1,i}^2\right) \rho_{k,i}^2 & \text{for } k \le i \le n-1. \end{cases}$$

Proof. Directed line networks have a diagonal controllability Gramian, $\mathscr{W}_{i,i+1}^k = 0$ for all i. By using (6), we know $\mathscr{W}_{ii}^k = 0$ for $1 \le i \le k-1$ which, when combined with Theorem 3, implies that $\gamma_{i,i+1}^k = 0$. For $i = k-1$, we have $\mathscr{W}_{k-1,k-1}^k = 0$ and $\mathscr{W}_{kk}^k = 1$, so $\gamma_{i,i+1}^k = c_{k-1,k}^2$. Finally, from (6), for $k \le i \le n-1$, we have $\mathscr{W}_{i+1,i+1}^k = a_{i+1,i}^2 \mathscr{W}_{ii}^k = a_{i+1,i}^2 \rho_{k,i}^2$ and the result follows from Theorem 3. □

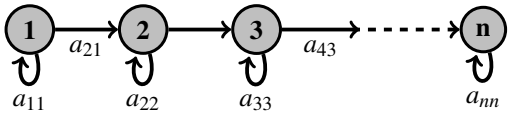

Fig. 2: A directed line network with n nodes.

B. Continuous-Time Directed Line Networks

Next, we consider directed line networks following continuous-time dynamics and having self-loops i.e., $a_{ii} < 0$ for all i. Given the lower triangular structure of the adjacency matrix, the condition $a_{ii} < 0$ ensures the stability of the network dynamics. Before proceeding to the derivation of edge flow vulnerabilities for directed line networks, we derive analytical relationships between the elements of the continuous-time controllability Gramian matrix.

Theorem 5. *(Analytical expressions for Gramian matrix elements). Consider a directed line network of n nodes with stable continuous-time dynamics* (1b) *and input node k. Then the elements of the controllability Gramian are given by,*

$$\mathscr{W}_{ii}^k = 0,\ \mathscr{W}_{ij}^k = \mathscr{W}_{ji}^k = 0 \text{ for } 1 \le i \le k,\ i \le j \le n,$$

$$\mathscr{W}_{kk}^k = \frac{-1}{2a_{kk}},\ \mathscr{W}_{kj}^k = \frac{-a_{j,j-1}\mathscr{W}_{k,j-1}^k}{\beta_{kj}} \text{ for } k \le j \le n,$$

$$\mathscr{W}_{ii}^k = \frac{-a_{i,i-1}\mathscr{W}_{i-1,i}^k}{a_{ii}},\ \mathscr{W}_{ij}^k = \frac{-\left(a_{i,i-1}\mathscr{W}_{i-1,j}^k + a_{j,j-1}\mathscr{W}_{i,j-1}^k\right)}{\beta_{ij}},$$

for $k+1 \le i \le n,\ i \le j \le n$, *where* $\beta_{ij} = a_{ii} + a_{jj}$.

Proof. As the controllability Gramian is symmetric, we just compute the upper triangular part. From the continuous-time Lyapunov equation (5b) for directed line networks and input node k, with $S = A\mathscr{W}^k + \mathscr{W}^k A^\top$, we get

$$\begin{aligned} S_{ij} &= 2a_{11}\mathscr{W}_{11}^k \text{ for } i = j = 1, \\ &= \beta_{1j}\mathscr{W}_{1j}^k + a_{j,j-1}\mathscr{W}_{i,j-1}^k \text{ for } i = 1,\ 2 \le j \le n, \\ &= 2a_{ii}\mathscr{W}_{ii}^k + 2a_{i,i-1}\mathscr{W}_{i-1,i}^k, \text{ for } 2 \le k \le i = j \le n, \\ &= \mathscr{W}_{i-1,j}^k a_{i,i-1} + \mathscr{W}_{i,j-1}^k a_{j,j-1} + \mathscr{W}_{ij}\beta_{ij}, \\ &\text{for } 2 \le k \le i \le n,\ i+1 \le j \le n. \end{aligned}$$

The right-hand side of the Lyapunov equation for the nodal input at node k is $-\bar{e}_k \bar{e}_k^\top$, which is a matrix whose only non-zero element is at the position (k,k) with value -1. Using this fact, $S_{kk} = -1$ and all other elements of the upper-triangular matrix $S_{ij} = 0$. We solve these linear equations for the Gramian elements to get the required result. □

Note that unlike the discrete-time case, the continuous-time controllability Gramian for stable directed line networks is not a diagonal matrix. Thus, the analytical expressions for the edge flow vulnerabilities in terms of the edge weights are complicated for any general edge $i \to i+1$. However, for the edges adjacent to the input node, the flow vulnerability in terms of the edge weights is computed using Theorem 6.

Theorem 6. *(Analytical expressions for flow vulnerabilities for edges adjacent to input node). Consider a directed line network of n nodes with stable continuous-time dynamics* (1b) *and input node k. Then for the edges adjacent to the input node, we have*

$$\gamma^k_{k-1,k} = \frac{-c^2_{k-1,k}}{2a_{kk}}, \quad for \quad 2 \le k \le n,$$

$$\gamma^k_{k,k+1} = \frac{-c^2_{k,k+1}}{2a_{kk}}\left(1 + \frac{a^2_{k+1,k}}{a_{k+1,k+1}\beta_{k+1,k}} + \frac{2a_{k+1,k}}{\beta_{k+1,k}}\right).$$

Proof. This can be proved by substituting $i = k-1$, $j = k$ and $i = k$, $j = k+1$ respectively in Theorem 5. □

When all the edge weights are equal in magnitude, i.e., $a_{i+1,i} = a$ and $a_{ii} = -a$ with $a > 0$, then by using Theorem 5 one can prove $\mathscr{W}^k_{i+1,i+1} = \mathscr{W}^k_{i,i+1}$. This results in $\gamma^k_{i,i+1} = c^2_{i,i+1}(\mathscr{W}^k_{ii} - \mathscr{W}^k_{i,i+1})$. Even with this simplification, obtaining a general analytical expression for $\gamma^k_{i,i+1}$ in terms of a is still difficult. However, from numerical experiments, we observe that as one moves away from the input node k along the directed line, $\gamma^k_{k+i,k+i+1}$ decreases as 2^s, where $s \ge 2i$ for $i = 1, \ldots, n$. Consequently, the influence of the nodal impulse on the flows along the directed line is expected to decrease significantly with the distance from the input node.

V. Numerical Experiments

In this section we consider two examples to illustrate our theory and demonstrate its efficacy. We use the maximum flow deviation during the time evolution of the network dynamics as a benchmark for evaluation. This captures the transient effects of impulse nodal inputs, which are often omitted when only sequential steady states are analyzed.

A. 7-Node Directed Line Network

Consider a family of $7-$node networks with the following edge weights: $a_{21} = 0.7$, $a_{32} = 0.8$, $a_{43} = 0.9$, $a_{54} = 0.6$, $a_{65} = 0.7$, $a_{76} = 0.5$. For networks with discrete-time dynamics we have no self-loops, while we consider self-loops with $a_{ii} = -1$ for all i, when the system follows continuous-time dynamics. We use a nodal impulse input with $u = 3$ for analyzing both the discrete/continuous-time dynamics.

(i) Discrete-time dynamics: Using Theorem 3, we first compute the VM matrix as tabulated in Table II. Next, we numerically simulate the dynamics until the iteration $T = 100$. We compute the maximum absolute deviation in flow ($\mathscr{F}_{ij} = \max |F_{ij}(t)|$) on each edge when the input is applied at different nodes. We then sum these maximum flow deviations to quantify the impact of a nodal impulse on the network. These results are tabulated in Table III. Note that the largest flow deviation occurs when the input is applied at node 2, which is also the node with the maximum nodal influence. This makes node 2 an ideal site for an impulse input attack.

k	γ_{12}	γ_{23}	γ_{34}	γ_{45}	γ_{56}	γ_{67}	ν_k
1	0.73	0.51	0.46	0.12	0.07	0.01	1.91
2	0.49	1.05	0.94	0.25	0.14	0.03	2.90
3	0	0.64	0.47	0.40	0.21	0.05	2.76
4	0	0	0.81	0.49	0.26	0.06	1.62
5	0	0	0	0.36	0.73	0.15	1.24
6	0	0	0	0	0.49	0.31	0.80
7	0	0	0	0	0	0.25	0.25

TABLE II: VM, nodal influence ν_k for discrete-time dynamics.

k	$\mathscr{F}_{12}$	$\mathscr{F}_{23}$	$\mathscr{F}_{34}$	$\mathscr{F}_{45}$	$\mathscr{F}_{56}$	$\mathscr{F}_{67}$	$\sum \mathscr{F}^k_{ij}$
1	2.10	1.68	1.51	0.91	0.64	0.32	7.15
2	2.10	2.40	2.16	1.29	0.91	0.45	9.32
3	0	2.40	2.70	1.62	1.13	0.57	8.42
4	0	0	2.70	1.80	1.26	0.63	6.39
5	0	0	0	1.80	2.10	1.05	4.95
6	0	0	0	0	2.10	1.50	3.60
7	0	0	0	0	0	1.50	1.50

TABLE III: Max flow deviation matrix for discrete-time dynamics.

(ii) Continuous-time dynamics: In this case, we have self-loops at each node with a negative edge weight. We follow a similar approach as in the discrete-time case. For numerical simulations, we use the MATLAB solver '*ode45*' with a time-span $[0,\ 100]$ for computing the edge flow deviations. Our results are tabulated in Tables IV and V.

k	γ_{12}	γ_{23}	γ_{34}	γ_{45}	γ_{56}	γ_{67}	ν_k
1	0.13	0.03	0.01	0.00	0.00	0.00	0.17
2	0.25	0.17	0.03	0.01	0.00	0.00	0.46
3	0	0.32	0.21	0.03	0.00	0.00	0.56
4	0	0	0.41	0.10	0.01	0.00	0.52
5	0	0	0	0.18	0.13	0.01	0.32
6	0	0	0	0	0.25	0.08	0.33
7	0	0	0	0	0	0.13	0.13

TABLE IV: VM, nodal influence ν_k for continuous-time dynamics.

k	$\mathscr{F}_{12}$	$\mathscr{F}_{23}$	$\mathscr{F}_{34}$	$\mathscr{F}_{45}$	$\mathscr{F}_{56}$	$\mathscr{F}_{67}$	$\sum \mathscr{F}^k_{ij}$
1	0.68	0.20	0.10	0.06	0.03	0.02	1.09
2	0.80	0.75	0.25	0.12	0.05	0.03	2.00
3	0	0.94	0.84	0.22	0.09	0.04	2.13
4	0	0	1.06	0.61	0.16	0.06	1.89
5	0	0	0	0.71	0.69	0.15	1.55
6	0	0	0	0	0.82	0.52	1.34
7	0	0	0	0	0	0.57	0.57

TABLE V: Max flow deviations for continuous-time dynamics.

From the last column of Table IV, node 3 has the highest influence on the edge flow deviations, as confirmed too by the last column of Table V. This is consistent with the result in Theorem 3. For a particular nodal input, the edge flow deviation as well as its vulnerability decreases as one moves away from the node in both discrete and continuous-time cases. The above simulation results also highlight that, even though the discrete-time, continuous-time cases have the same directed line edges, they have different influential input locations. We repeated the simulations for $u = \{-10, -3, -1, 1, 10\}$, leading to identical results.

(iii) Weak directed line networks: Consider the directed line network following the continuous-time dynamics in *(ii)*. To this network, we add 10 new edges at randomly selected locations having edge weights (again selected randomly) from the set $(0,\ 0.1]$. As the edge weights along the pure directed line ($i \to i+1$) are significantly larger than the newly added edge weights, we refer to such networks as 'weak directed line networks'. We construct 1000 such network cases. Using the same u and time span as in *(ii)*, we perform numerical simulations to compute the edge flow deviations. With this information for each network, we order its nodes according to decreasing $\sum \mathscr{F}_{ij}^k$. We observe that node 3 is the most influential node in 861 cases, second-most influential in 138 cases, and third-most influential in 1 case. Thus, Theorem 3, even without the exact structure of weak directed line networks (since Table IV is computed for the directed line case), helps identify the most influential node with reasonable accuracy.

B. Random Erdős-Rényi Networks

In this section, we underscore the efficacy of our proposed VM metric and its utility on 1000 random Erdős-Rényi (ER) networks [24], each having $n = 100$ nodes and following continuous-time dynamics. For each network, we select the edge locations with a probability of 0.4. The weight of each edge is selected as a random scalar, drawn from the standard normal distribution (using the MATLAB function '*randn*'). We add self-loops of weight -7 at each node of the network. This ensures that the real part of each eigenvalue of the matrix A of each network is less that -0.1, thereby making the dynamics stable. We numerically simulate the dynamics for each network as in Example V-A *(ii)* for a time span of $[0,\ 50]$ and various input values $u = \{-30,\ -15,\ -3,\ 3,\ 15,\ 30\}$. For each u and each network, we compute the flow deviations $\mathscr{F}_{ij}$ and arrange the input nodes in descending order of $\sum \mathscr{F}_{ij}^k$. Next, for each ER network, we determine the node with the largest vulnerability using the VM computed from Theorem 3. We observe that, for each case, the most influential node (computed using Theorem 3) features in the top three influential nodes computed using the flow deviation simulations in around 95% ($1^{\text{st}} - 72\%,\ 2^{\text{nd}} - 16\%,\ 3^{\text{rd}} - 7\%$) of the cases. This provides evidence of the vulnerability matrix as an effective tool to identify vulnerable nodal sites for impulse attacks.

VI. Conclusions

We have analyzed the effect of impulse inputs on edge flows in networks with stable linear invariant discrete-time or continuous-time dynamics. Next, we introduced the notion of vulnerability matrix, a map of first-order effects on the flow of each edge due to an impulse input at each node of the network, and described its efficacy in identifying vulnerable nodes. Our analysis captures the transient effects of impulse nodal inputs on edge flows and quantifies them in terms of the controllability Gramian. We have provided explicit expressions for the entries of the vulnerability matrix for the class of directed line networks with positive edge weights and stable (discrete/continuous)-time dynamics. Numerical simulations have illustrated our approach and examined its usefulness in identifying the maximum flow deviation in the network. Future work will extend the analytical characterization of the vulnerability matrix to more general graph topologies, explore other metrics (e.g., $\mathscr{H}_\infty$) to measure vulnerability, extend our treatment to step inputs, and apply the results to the identification/prevention of cascading failures.

References

[1] F. Bullo, *Lectures on Network Systems*, 1st ed. Kindle Direct Publishing, 2022.

[2] F. Bullo, J. Cortés, and S. Martinez, *Distributed Control of Robotic Networks*, ser. Applied Mathematics Series. Princeton University Press, 2009.

[3] M. O. Jackson, *Social and Economic Networks*. Princeton University Press, 2010.

[4] E. Estrada, *The Structure of Complex Networks: Theory and Applications*. Oxford University Press, 2012.

[5] M. Newman, *Networks: An Introduction*. Oxford University Press, 2018.

[6] P. V. Chanekar and J. Cortés, "Encoding impact of network modification on controllability via edge centrality matrix," *IEEE Transactions on Control of Network Systems*, pp. 1–12, 2022.

[7] F. Pasqualetti, S. Zampieri, and F. Bullo, "Controllability metrics, limitations and algorithms for complex networks," *IEEE Transactions on Control of Network Systems*, vol. 1, no. 1, pp. 40–52, 2014.

[8] T. H. Summers, F. L. Cortesi, and J. Lygeros, "On submodularity and controllability in complex dynamical networks," *IEEE Transactions on Control of Network Systems*, vol. 3, no. 1, pp. 91–101, 2016.

[9] P. V. Chanekar, E. Nozari, and J. Cortés, "Energy-transfer edge centrality and its role in enhancing network controllability," *IEEE Transactions on Network Science and Engineering*, vol. 8, no. 1, pp. 331–346, 2020.

[10] G. Lindmark and C. Altafini, "Centrality measures and the role of non-normality for network control energy reduction," *IEEE Control Systems Letters*, vol. 5, no. 3, pp. 1013–1018, 2020.

[11] S. Pushpak, A. Diwadkar, M. Fardad, and U. Vaidya, "Vulnerability analysis of large-scale dynamical networks to coordinated attacks," in *Australian Control Conference*, Canberra, Australia, 2014, pp. 89–94.

[12] I. Shames, F. Farokhi, and T. H. Summers, "Security analysis of cyber-physical systems using H_2 norm," *IET Control Theory & Applications*, vol. 11, no. 11, pp. 1749–1755, 2017.

[13] M. Siami and N. Motee, "Fundamental limits on robustness measures in networks of interconnected systems," in *IEEE Conference on Decision and Control*, Firenze, Italy, 2013, pp. 67–72.

[14] Q. Huang, Y. Yuan, J. Gonçalves, and M. A. Dahleh, "H_2- norm based network volatility measures," in *American Control Conference*, Portland, OR, USA, 2014, pp. 3310–3315.

[15] F. Pasqualetti, S. Zhao, C. Favaretto, and S. Zampieri, "Fragility limits performance in complex networks," *Scientific Reports*, vol. 10, no. 1, pp. 1–9, 2020.

[16] S. Soltan, D. Mazauric, and G. Zussman, "Analysis of failures in power grids," *IEEE Transactions on Control of Network Systems*, vol. 4, no. 2, pp. 288–300, 2015.

[17] D. Manik, M. Rohden, H. Ronellenfitsch, X. Zhang, S. Hallerberg, D. Witthaut, and M. Timme, "Network susceptibilities: Theory and applications," *Physical Review E*, vol. 95, no. 1, p. 012319, 2017.

[18] B. Schäfer, D. Witthaut, M. Timme, and V. Latora, "Dynamically induced cascading failures in power grids," *Nature Communications*, vol. 9, no. 1, pp. 1–13, 2018.

[19] F. Dörfler, M. Chertkov, and F. Bullo, "Synchronization in complex oscillator networks and smart grids," *Proceedings of the National Academy of Sciences*, vol. 110, no. 6, pp. 2005–2010, 2013.

[20] C. T. Chen, *Linear System Theory and Design*, 3rd ed. New York, NY, USA: Oxford University Press, Inc., 1998.

[21] K. Ogata, *Modern Control Engineering*. Prentice Hall, NJ, 2010, vol. 5.

[22] K. Zhou, J. Doyle, and K. Glover, *Robust and Optimal Control*. Prentice Hall, NJ, 1995.

[23] S. Zhao and F. Pasqualetti, "Discrete-time dynamical networks with diagonal controllability Gramian," *IFAC-PapersOnLine*, vol. 50, no. 1, pp. 8297–8302, 2017.

[24] P. Erdös and A. Rényi, "On the evolution of random graphs," *Publications of the Mathematical Institute of the Hungarian Academy of Sciences*, vol. 5, pp. 17–61, 1960.